Amino acid deaminase outperforms transaminase in α-keto acid production from amino acids

Nasuno, Ryo ; Kudo, Hisashi ; Fushimi, Keiji ; Hidese, Ryota ; Kondo, Akihiko ; Hasunuma, Tomohisa

(Citation)
Metabolic Engineering,96:234-242

(Issue Date)
2026-07

(Resource Type)
journal article

(Version)
Version of Record

(URL)
https://hdl.handle.net/20.500.14094/0100503505

Metabolic Engineering 96 (2026) 234–242

Contents lists available at ScienceDirect

Metabolic Engineering

journal homepage: www.elsevier.com/locate/meteng

Amino acid deaminase outperforms transaminase in α-keto acid production from amino acids

Ryo Nasuno [a], Hisashi Kudo [a], Keiji Fushimi [b], Ryota Hidese [a], Akihiko Kondo [a,b,c], Tomohisa Hasunuma [a,b,c,*]

[a] *Engineering Biology Research Center, Kobe University, 1-1 Rokkodai, Nada, Kobe, 657-8501, Japan*
[b] *Graduate School of Science, Technology, and Innovation, Kobe University, 1-1 Rokkodai, Nada, Kobe, Hyogo, 657-8501, Japan*
[c] *Research Center for Sustainable Resource Science, RIKEN, 1-7-22 Suehiro, Tsurumi, Yokohama, Kanagawa, 230-0045, Japan*

ARTICLE INFO

Keywords:
Deaminase
Transaminase
α-Keto acid
α-Amino acid
Auxin
Microbial production

ABSTRACT

α-Keto acids are central metabolic intermediates that serve as precursors for a broad range of valuable compounds, including alcohols, organic acids, and alkanes. Therefore, efficient biosynthesis of α-keto acids from α-amino acids is essential for microbial production of α-keto acids-derived products. While transaminases have traditionally been employed for this conversion, their dependence on α-ketoglutarate and reversibility can impose metabolic burdens and limit yield. Recently, amino acid deaminases (AADs) have been used for conversion of amino acids to α-keto acids, because AADs catalyze irreversible oxidative deamination without any cosubstrate and thus may offer advantages for α-keto acid production. Here, we experimentally demonstrated the superiority of AADs over transaminases in amino acid-to-α-keto acid conversion for the first time, using the production of indole-3-acetic acid from tryptophan as a case study. *Escherichia coli* cells expressing AAD genes from *Proteus myxofaciens* or *P. mirabilis* exhibited higher production of indole-3-acetic acid and indole-3-pyruvic acid, which is a direct product from tryptophan and an intermediate for indole-3-acetic acid production, than transaminases. Our kinetic analysis revealed that AADs exhibited higher affinity towards tryptophan than transaminases, contributing to higher production rate. This is the first report to demonstrate the superiority of AADs over transaminases for α-keto acids production. Furthermore, AADs showed better performance in the bioconversion of leucine, valine, and phenylalanine to their corresponding α-keto acids than transaminases. These findings establish AADs as promising biocatalysts for α-keto acid synthesis, supporting their use in pathway design for bioproduction of α-keto acid-derived compounds.

1. Introduction

Microbial cell factories have emerged as powerful platforms for the sustainable production of a wide variety of valuable compounds, including fuels, natural bioactive chemicals, pharmaceuticals, and commodity chemicals (Cowan et al., 2023). Advances in metabolic engineering and synthetic biology have enabled microorganisms such as *Escherichia coli*, *Corynebacterium glutamicum*, and *Saccharomyces cerevisiae* to efficiently synthesize products like isoamyl acetate, isobutanol, 1,3-propanediol, L-glutamate, and an anti-malarial agent artemisinin (Rumpl et al., 2025; Smith and Chekan, 2023; Wendisch et al., 2016; Wong and Jantama, 2022). Some of these compounds are produced even on an industrial scale.

In metabolic pathways for bioproduction, several molecules function as metabolic hubs that serve as branching points in microbial metabolism, enabling the synthesis of a diverse range of products. α-Keto acids (KAs) are important metabolic hubs, which are highly related to metabolism of several α-amino acids (AAs) (Fig. 1A). KAs can be converted to their corresponding aldehydes by decarboxylase, and then reduced to alcohols by alcohol dehydrogenase in Ehrlich pathway (Atsumi et al., 2008). An intermediate aldehyde is also metabolized to carboxylic acids or alkanes by aldehyde dehydrogenase or aldehyde deformylating oxygenase, respectively (Atsumi et al., 2010; Ha et al., 2025; Marsh and Waugh, 2013; Zhang et al., 2011). For example, pyruvate has been used as a substrate to produce isobutanol through α-ketoisovaleric acid (KIV) formation in bacteria and yeast (Gu et al., 2023; Hasegawa et al., 2020; Wess et al., 2019). α-Ketoisocapronic acid (KIC) is used as a substrate to synthesize isoamyl alcohol, which is

---

[*] Corresponding author. Engineering Biology Research Center, Kobe University, 1-1 Rokkodai, Nada, Kobe 657-8501, Japan.
E-mail address: hasunuma@port.kobe-u.ac.jp (T. Hasunuma).

https://doi.org/10.1016/j.ymben.2026.04.001
Received 29 October 2025; Received in revised form 24 March 2026; Accepted 1 April 2026

suitable to be an additive or alternative to gasoline (Tashiro et al., 2015). 2-Phenylethanol produced from phenylpyruvate (Ppyv) is an important flavoring agent (Zheng et al., 2024). The most common natural plant hormone of the auxin class, indole-3-acetic acid (IAA) is synthesized from tryptophan through indole-3-pyruvic acid (IPA) as an intermediate (Fig. 1B) (Guo et al., 2019).

Synthesis of KAs from primary metabolites like AAs would be one of promising strategies for efficient production of various valuable compounds derived from KAs (Fig. 1A). Enzymes, which catalyze the conversion of AAs to KAs, include transaminase (TA, EC 2.6.1.-), amino acid dehydrogenase (AADH, EC 1.4.1.-), amino acid oxidase (AAO, EC 1.4.3.2), and amino acid deaminase (AAD, EC 1.4.99. B3) (Fig. 2). TA is a large family of pyridoxal 5′-phosphate (PLP)-dependent enzymes and catalyzes the reversible transamination reaction between one AA and one KA, thus TA requires α-ketoglutarate (αKG) as a receptor of amino group from its substrate AAs (Koper et al., 2022). AADH, AAO, and AAD catalyze similar reactions, which is oxidative deamination. All three enzymes harbor FAD as a cofactor and oxidize amino group in their substrate AAs to imine group, followed by hydrolysis to carbonyl group (Pollegioni et al., 2013; Schriek et al., 2009). AADH, whose oxidative deamination reaction is reversible, dehydrogenizes the amino group with the aid of $NAD(P)^+$ (Li et al., 2012; Smith et al., 2019). AAO oxidizes AAs, in which molecular oxygen functions as an electron acceptor, to generate hydrogen peroxide as a byproduct, which is potential to be toxic when heterologously expressed in a conventional microbe for bioproduction (Pollegioni et al., 2013). AAD, which has a transmembrane domain in its N-terminus to associate cellular membrane, oxidizes AAs to KAs using a cytochrome *b*-like membrane protein as a direct electron acceptor (Molla et al., 2017).

Among them, TAs are best characterized and thus have been often utilized for KA production from AA, especially aromatic amino acids like tryptophan. For example, an aspartate transaminase-encoding gene *aspC* from *E. coli* or *S. cerevisiae* aromatic transaminase gene *ARO8* have been expressed in *E. coli* (Guo et al., 2019; Romasi and Lee, 2013). The recombinant strains have successfully produced IAA in combination with enzymes responsible for further reaction like decarboxylase and aldehyde dehydrogenase (Guo et al., 2019; Romasi and Lee, 2013). TAs like β-alanine-pyruvate transaminase or ω-transaminases, which use β-amino acids or ω-amino acids as an amino donor, respectively, have also been employed for the production of valuable compounds (Liu et al., 2025; Nieto-Domínguez et al., 2024).

Recently, AAD, one of the other three enzymes to catalyze oxidative deamination, has been applied to synthesize KAs from AAs. *E. coli* strain expressing AAD gene derived from *Proteus mirabilis* or *Proteus vulgaris* was used for the conversion of phenylalanine to phenylpyruvate or methionine to α-keto-γ-methylthiobutyric acid, respectively, as a whole-cell biocatalyst (Hossain et al., 2014; Hou et al., 2016).

One of the reasons why AADs are thought to be better than TAs for KA production would be that TAs require αKG as an amino group receptor for their transamination reactions, which is an important metabolic intermediate involved in central metabolic pathway like TCA cycle, as researchers mentioned (Song et al., 2016). An excess rate of transamination reactions is likely to lead to a reduction in αKG level, causing metabolic imbalances. However, there has been no experimental evidence to directly demonstrate the performance of AADs is superior to TAs in KA synthesis under controlled experimental conditions. Such comparative analysis is essential to inform rational enzyme selection for biosynthetic pathway design and industrial-scale production.

In this study, we experimentally examined the hypothesis that AADs outperform TAs in the production of KAs from AAs, using the production of IAA from tryptophan as a case study. The *E. coli* cells expressing AAD genes exhibited higher production levels of not only IPA but also IAA from tryptophan than those expressing TA genes. Our kinetic analysis of purified enzymes demonstrated that AAD has higher affinity to tryptophan than TAs. These results suggest that not only αKG requirement but also the difference of substrate affinity make AADs better than TAs as KA producing enzymes from AA.

2. Methods

2.1. Strains, plasmids, and medium

The *Escherichia coli* strain DH5α (F^-, Φ80d*lacZ*ΔM15, Δ(*lacZYA*-

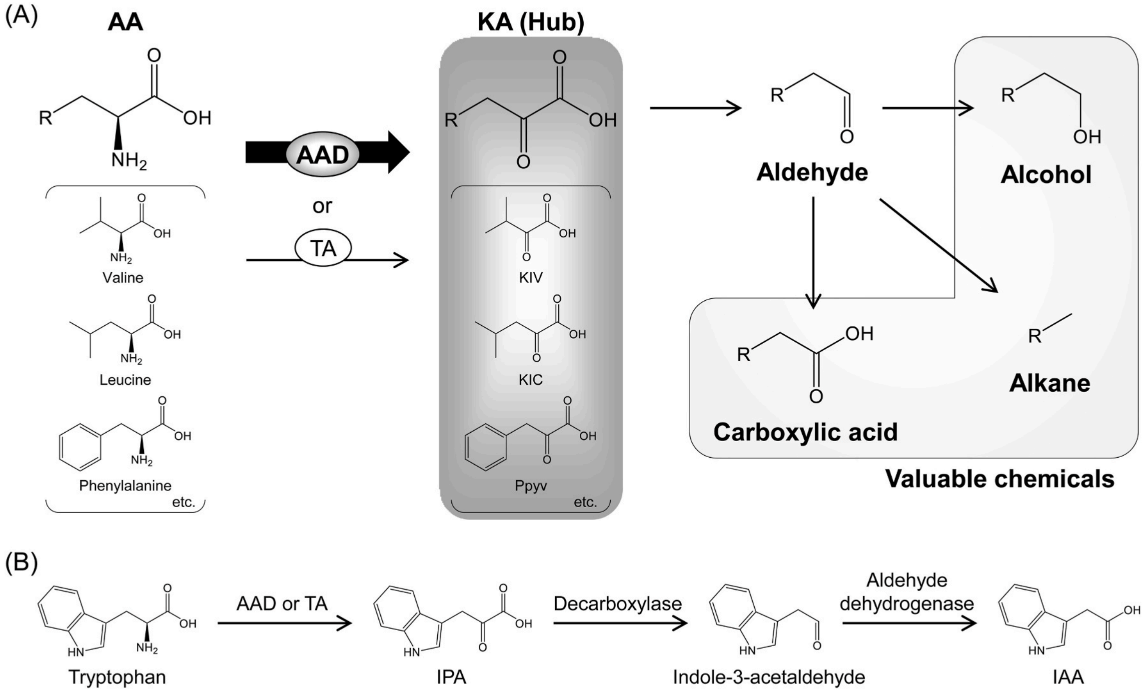

Fig. 1. Bioproduction using KAs as hubs. (A) Production of various valuable compounds *via* the conversion from AAs to KAs. (B) IAA production pathway from tryptophan through three enzymatic reactions.

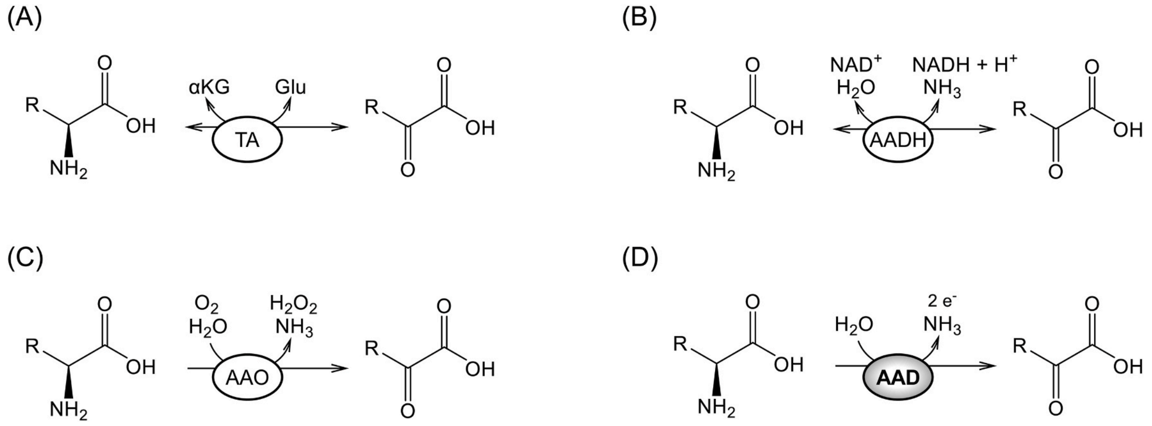

Fig. 2. Four enzymes catalyzing the conversion from AAs to KAs. (A) transaminase (TA), (B) amino acid dehydrogenase (AADH),(C) amino acid oxidase (AAO), (D) amino acid deaminase (AAD) synthesizes KAs from AAs.

argF)U169, *deoR*, *recA*1, *endA*1, *hsdR*17 ($r_K^- m_K^+$), *phoA*, *supE*44, λ^-, *thi*-1, *gyrA*96, *relA*1) or BL21 (DE3) (F^- *omp*T *hsd*S_B ($r_B^- m_B^-$) *gal dcm* (DE3)) were used for the plasmid construction or enzyme production, respectively. AADs from *Proteus myxofaciens* (PmyxAAD, NCBI Reference Sequence ID: WP_066749310.1) and *P. mirabilis* (PmirAAD, GenBank ID: HBC6705881.1) were used in this study. An indolepyruvate decarboxylase IpdC from *Enterobacter cloacae* (GenBank ID: ADF63262.1) and an aldehyde dehydrogenase PuuC from *E. coli* BL21 (DE3) strain (GenBank ID; QNG32311.1) were also used for IAA production. The two AAD-encoding genes, IpdC-encoding gene (*ipdC*), and PuuC-encoding gene (*puuC*) were synthesized by Gene Synthesis Service from GenScript Biotech Corporation with codon optimization for *E. coli*.

The AAD-encoding genes, *PmyxAAD* and *PmirAAD*, were cloned into the plasmid pET28a (+) (Novagen) or pRSFDuet-1 (Novagen) by PCR and InFusion reaction (Clontech) following the manufacturer's protocol, generating the resultant plasmid pET-PmyxAAD, pET-PmirAAD, pRSF-PmyxAAD, and pRSF-PmirAAD. The AAD-encoding genes were also cloned into pETDuet-1 (Novagen), in which the coding regions for N-terminal 27 amino acids of PmyxAAD and N-terminal 29 amino acids of PmirAAD were removed, by PCR and InFusion reaction, resulting in the plasmid pET-PmyxAADdN27 and pET-PmirAADdN29. The TA-encoding genes from *E. coli* (*aspC*) and *Saccharomyces cerevisiae* (*ARO8*), which were amplified by PCR from the genome of *E. coli* MG1655 strain and *S. cerevisiae* BY4741 strain, were cloned into pET28a (+) and pRSFDuet-1 by PCR and InFusion reaction, generating the plasmid pET-aspC, pET-ARO8, pRSF-aspC, and pRSF-ARO8. *ipdC* and *puuC* were cloned into a multi cloning site-1 and -2 of the plasmid pACYCDuet-1 (Novagen) by PCR and InFusion reaction, respectively, resulting in the plasmid pACYC-ipdC-puuC. The *tyrB* gene encoding an aromatic amino acid transaminase TyrB or the *ilvE* gene encoding a branched chain amino acid transaminase IlvE was cloned from the genome of *E. coli* MG1655 strain into the pRSFDuet-1 plasmid, which generates the plasmid pRSF-tyrB or pRSF-ilvE, respectively.

LB medium consisting of 0.5% yeast extract, 1% tryptone, and 1% NaCl, or M9CA medium, which was prepared using 5 × BD Difco™ M9 Minimal Salts (Becton Dickinson) following the manufacturer's procedure, supplemented with 2% of Acid Hydrolysate of Casein (Solabia Biokar Diagnostics) were used to culture *E. coli* strains.

The plasmids used in this study were listed in Table S1.

2.2. Bioconversion of AA to α-keto acid

The *E. coli* BL21 (DE3) strain harboring pET28a (+), pET-PmyxAAD, pET-PmirAAD, pET-aspC, or pET-ARO8 was cultured in LB medium supplemented with 100 μg/mL carbenicillin at 37 °C overnight. The fresh LB + kanamycin medium inoculated with the 1/100 volume of preculture was cultivated at 37 °C for 4.5 h, and then 100 μM isopropyl-β-D-thiogalactopyranoside (IPTG) was added, followed by further incubation at 37 °C for 18 h for gene overexpression. After induction, cells were pelleted, washed with, and suspended in 100 mM Tris-HCl (pH 7.5). Cell suspensions were incubated at 30 °C for 72 h in the presence of 10 mM of tryptophan and 10, 20, or 50 mM of αKG. Supernatants after centrifugation of cell suspensions were subjected to high performance liquid chromatography (HPLC) analysis to determine the IPA concentration.

For the bioconversion from phenylalanine, leucine, and valine to Ppyv, KIC, and KIV, the *E. coli* BL21 (DE3) cells harboring the plasmid pACYCDuet-1 and pRSFDuet-1, pRSF-PmyxAAD, pRSF-PmirAAD, pRSF-tyrB, or pRSF-ilvE were cultured in LB + 25 μg/mL kanamycin and 10 μg/mL chloramphenicol overnight. The 1/100 volume of preculture was inoculated to fresh LB medium with kanamycin and chloramphenicol and then cultured at 37 °C for 3 h. The gene expression was induced by the addition of 100 μM IPTG at 37 °C for 24 h. Harvested cells were washed with and resuspended in 100 mM Tris-HCl (pH 7.5) and further incubated in the presence of 10 mM of AAs and 10, 20, or 50 mM of αKG at 30 °C for 24 h. Supernatants after centrifugation of cell suspensions were subjected to derivatization, followed by HPLC analysis.

2.3. Bioproduction of IAA from tryptophan

The *E. coli* BL21 (DE3) strain harboring the plasmid pACYC-ipdC-puuC and pRSF-PmyxAAD, pRSF-PmirAAD, pRSF-aspC, or pRSF-ARO8 were cultured in LB + 25 μg/mL kanamycin and 10 μg/mL chloramphenicol overnight. The fresh LB + kanamycin and chloramphenicol medium, which contained 5 mM of tryptophan and 5, 10, or 25 mM of αKG, inoculated with the 1/100 volume of preculture was cultivated at 37 °C for 4 h, and then 100 μM IPTG was added, followed by further incubation at 37 °C for 24 h. Supernatants after centrifugation to remove cells from culture was analyzed by HPLC.

2.4. Derivatization of α-keto acid for HPLC analysis

Samples containing Ppyv, KIC, or KIV were derivatized following the previous report with slight modifications (Fujiwara et al., 2020). Equal volume of samples and the derivatization solution, which consisted of 7.1 mM 1,2-diamino-4,5-methylenedioxybenzene dihydrochloride, 7% 2-mercaptoethanol, and 700 mM HCl, were mixed and incubated at 85 °C for 50 min. Subsequently, the resultant solutions were analyzed by HPLC after fivefold dilution with 87.5 mM NaOH. Serial dilutions of Ppyv, KIC, or KIV were derivatized in the same method to draw the standard curve.

2.5. HPLC

HPLC was performed using an HPLC system Nexera-i LC-2040C MT plus equipped with a fluorescence detector RF-20 A XS (Shimadzu). HPLC to quantify IPA was performed with a Kinetex 2.6 μm EVO C18 100 Å (100 mm × 2.1 mm) (Phenomenex) by the following gradient system with a flow rate of 0.4 mL/min, using 0.1% acetic acid and methanol as a solvent A and B (time, % of solvent A): 0 min, 90%; 1.2 min, 90%; 3 min, 65%; 7.2 min, 40%; 9.6 min, 40%; 9.61 min, 90%; 12 min, 90%. For IAA analysis, HPLC was performed with a Kinetex 2.6 μm C8 100 Å (100 mm × 2.1 mm) (Phenomenex) by the following gradient program with a flow rate of 0.4 mL/min, using 2.5% potassium acetate (pH 3.8) and 80% acetonitrile as a solvent A and B (time, % of solvent A): 0 min, 100%; 2 min, 100%; 10 min, 80%; 12 min, 50%; 13 min, 0%; 15 min, 0%; 15.01 min, 100%; 17 min, 100%. HPLC to determine the concentration of Ppyv, KIC, and KIV was conducted with a Kinetex 2.6 μm EVO C18 100 Å (100 mm × 2.1 mm) by the following gradient system with a flow rate of 0.6 mL/min, using 20 mM potassium phosphate (pH 2.5) and acetonitrile as a solvent A and B (time, % of solvent A): 0 min, 90%; 4 min, 90%; 15 min, 70%; 20 min, 70%; 20.01 min, 90%; 25 min, 90%.

2.6. Expression and purification of AAD and TA

The *E. coli* BL21 (DE3) strain harboring pET-PmyxAADdN27 was cultured in M9CA supplemented with 100 μg/mL carbenicillin and 200 μM riboflavin at 37 °C until OD600 = 0.6, and then the gene expression was induced with 100 μM IPTG at 18 °C for 18 h. Harvested cells were washed with and suspended in Buffer A consisting of 20 mM sodium phosphate (pH 7.4) and 500 mM NaCl, followed by cell disruption with sonication using an ultrasonic disruptor UD-200 (Tomy). Supernatant after centrifugation was subjected to affinity purification using Ni Sepharose™ 6 Fast Flow (Cytiva) following the previous report with slight modifications, in which 25 mM of imidazole was used to wash contaminant proteins from resin (Nasuno et al., 2013). Eluates containing high concentrations of protein were pooled and dialyzed against 20 mM HEPES-Na (pH 7.4) containing 150 mM NaCl and 5% glycerol, using Slide-A-Lyzer™ MINI Dialysis Devices, 20 K MWCO (ThermoFisher Scientific).

The TA production was induced as follows. The *E. coli* BL21 (DE3) strain harboring pACYCDuet-1 and pRSF-aspC or pRSF-ARO8 was cultured in LB medium containing 50 μg/mL kanamycin and 20 μg/mL chloramphenicol at 37 °C overnight. The preculture was inoculated to a fresh same medium and cultivated at 37 °C for 3 h, followed by the gene induction by 100 μM IPTG at 37 °C for 18 h. Harvested cells were washed with and suspended in 10 mM potassium phosphate (pH 7.5) and mixed with 1/9 volume of FastBreak™ Cell Lysis Reagent, followed by incubation at 4 °C for 30 min. Supernatant after centrifugation was used as a crude extract for following the TA activity assay. Cell pellets prepared by the same protocol were used for TA purification, following the same protocol as AAD, as described above.

The purified enzymes were subjected to SDS-PAGE, followed by Coomassie brilliant blue (CBB) staining to examine their purities. The protein level of AAD or TA in crude extract was estimated by SDS-PAGE and CBB staining, followed by densitometry using ImageJ (Schneider et al., 2012).

2.7. Enzymatic activity assay of AAD and TA using crude extract of *E. coli* cells

The solution containing 50 mM potassium phosphate (pH 7.5), 5 μM 1-methoxy-5-ethylphenazinium ethylsulfate (mPES) as an electron mediator, 10 μM resazurin whose reduced form emits fluorescence, AAs, and the purified enzymes were incubated and the fluorescence with an excitation wavelength of 553 nm and an emission wavelength of 598 nm over time, for AAD activity assay. Twenty-two kinds of AAs containing 20 proteinogenic AAs, ornithine, and citrulline were used as substrates to analyze the substrate selectivity of AADs at the concentration of 5 mM, except for tyrosine and tryptophan, for which the concentration was 2.5 mM. Kinetic analyses were performed using varied concentrations of tryptophan as a substrate.

The solution containing 50 mM potassium phosphate (pH 7.5), 5 mM tryptophan, 5 mM αKG, 10 μM PLP, and a crude extract was incubated and absorption at 327 nm was monitored over time, to determine the specific activity for TA. The varied concentrations of tryptophan and purified TA were used for kinetic analysis. Same solutions lacking a crude extract but containing various concentrations of IPA were prepared and absorption at 327 nm was measured to draw the standard curve to determine the IPA concentration.

The Michaelis-Menten constant K_m was determined using curve fitting with GraphPad Prism 9 (GraphPad Software).

3. Results

3.1. Bioconversion of tryptophan to IPA

First, the conversion of tryptophan to IPA was performed to examine the hypothesis described in the introduction (Fig. 1B). The *E. coli* cells expressing AAD gene or TA gene were incubated with 10 mM tryptophan and varied concentration of αKG (10, 20, or 50 mM) for 72 h at 30 °C and the production of IPA, which is a KA directly synthesized from tryptophan, was analyzed by HPLC (Fig. 3A). The result indicated that the *E. coli* cells producing PmyxAAD or PmirAAD synthesized more than 12 mM of IPA, regardless of αKG supplementation. On the other hand, cells harboring an empty vector, those producing an aspartate transaminase AspC derived from *E. coli*, and strain expressing *ARO8* gene encoding an aromatic transaminase from *S. cerevisiae* hardly synthesized IPA in the absence of αKG. When 10 mM of αKG was supplied, the IPA production level by the strain harboring an empty vector, expressing *aspC*, and expressing *ARO8* increased to 5, 8, or 8 mM, respectively. However, the IPA produced by these three strains did not increase significantly even though the αKG contents increased to 20 or 50 mM. These results indicate that AADs are more capable of converting tryptophan to IPA than TAs. Furthermore, the fact that cells expressing AAD genes synthesized more IPA than cells expressing TA genes even in the presence of excess αKG, and that αKG supplementation enhanced the IPA production in the strains expressing TA genes, suggests that AADs are superior to TAs for KA production *via* not only the αKG independence but also additional mechanisms.

Analyzing the protein level of each KA producing enzyme in *E. coli* by SDS-PAGE using whole cell extract, PmyxAAD and PmirAAD exhibited not only the band showing the theoretically predicted size of band but also the smaller size of band, which suggests the degradation of these AADs during this analysis (Fig. 3B). The protein quantification by densitometry suggested the relative protein level of full length PmyxAAD, full length PmirAAD, AspC, and Aro8 were 1.1, 1.0, 2.8, and 1.6, which suggests that the better capability of AADs for IPA production from tryptophan to TAs are not due to the protein level in cells.

To confirm that AspC and Aro8 were produced as functional proteins, the transaminase activity of each TA toward tryptophan was measured in crude extract of *E. coli* expressing *aspC* or *ARO8* (Fig. 4). As a result, the cells expressing *aspC* or *ARO8* exhibited a clear tryptophan transaminase activity. These indicate that both TAs, AspC and Aro8, were functionally produced in *E. coli* cell, even though their capacities to convert tryptophan to IPA were significantly less than AADs as shown in Fig. 3A.

3.2. Bioproduction of IAA from tryptophan

IAA production from tryptophan by three enzymatic reactions in *E. coli* was performed, in which IPA produced by AADs or TAs was further converted to IAA through decarboxylation by IpdC and

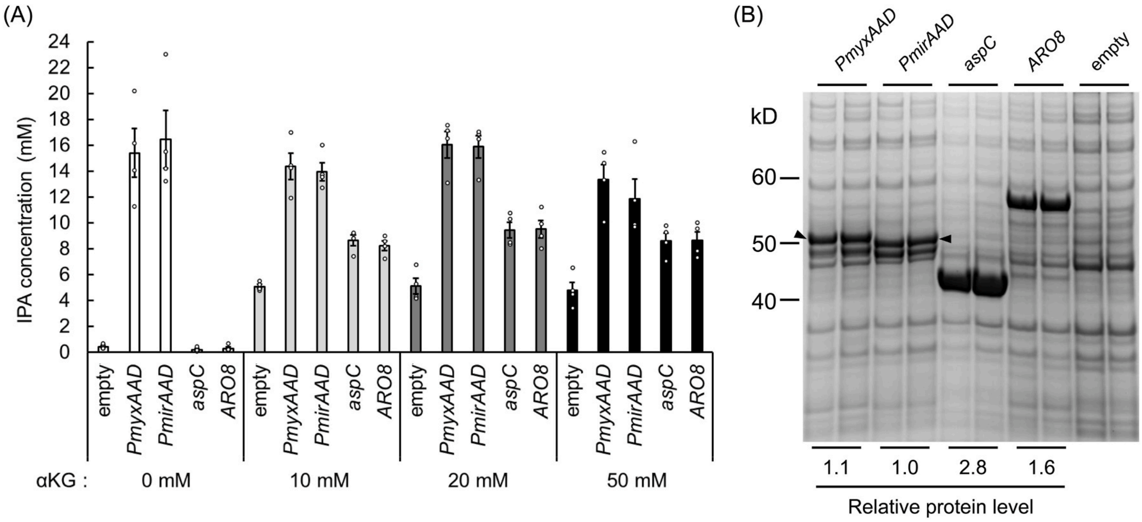

Fig. 3. Bioconversion of tryptophan to IPA by *E. coli* cells expressing AAD or TA genes. (A) IPA production in culture supernatant of *E. coli* strains over-expressing AAD or TA genes, in the presence or absence of αKG. Empty indicate the cells harboring an empty vector. The values are means and standard errors of at least four independent experiments. (B) The protein level of each enzyme was demonstrated by SDS-PAGE. Empty indicate the cells harboring an empty vector. The protein bands corresponding to full length of PmyxAAD and PmirAAD were indicated by arrowheads. The protein level of each enzyme of interest (full length PmyxAAD, full length PmirAAD, AspC, and Aro8) was quantified by densitometry using ImageJ and the relative protein levels were indicated.

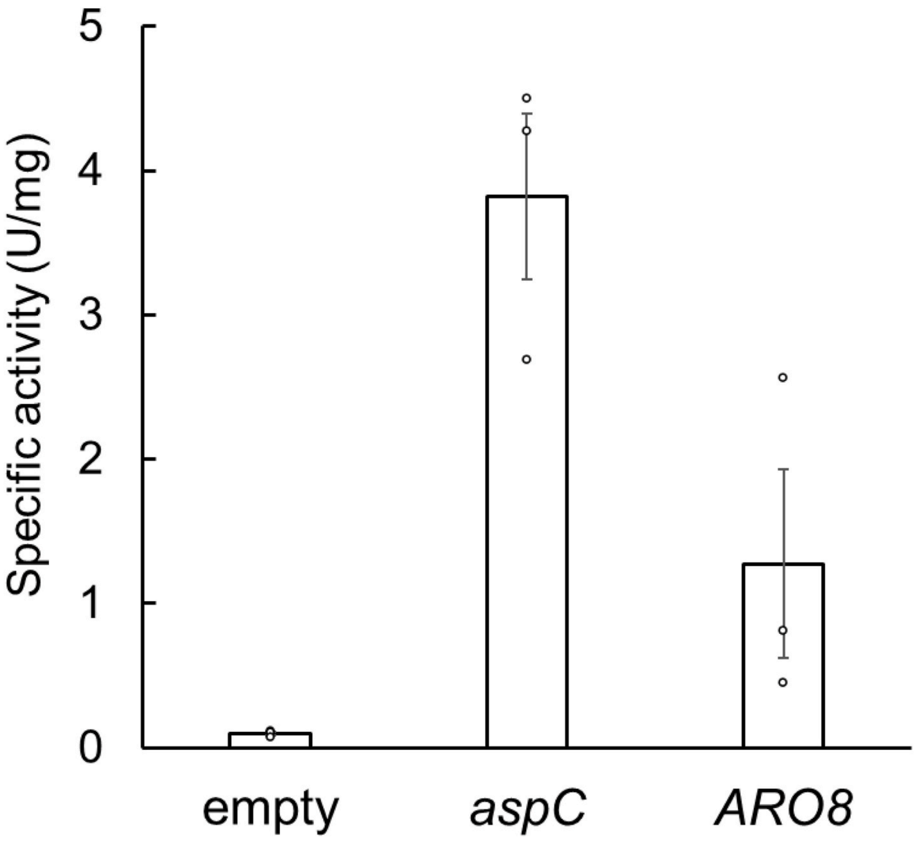

Fig. 4. TAs activities in crude extract of *E. coli* cells expressing TA genes. Specific activity of crude extract from each strain towards tryptophan. Empty indicate the cells harboring an empty vector. The values are means and standard errors of three independent experiments.

dehydrogenation by PuuC (Figs. 1B and 5). The cells expressing *PmyxAAD* or *PmirAAD* produced around 200 or 170 μM IAA, on the other hand, the cells expressing *aspC* or *ARO8* synthesized 20 μM IAA, which was comparable to the IAA production by the strain harboring an empty vector, under the condition without αKG supplementation. When 5 mM of αKG was added to medium, the production level of IAA by *E. coli* harboring an empty vector or expressing TA-encoding genes increased to almost 5-folds. Importantly, the IAA production levels by the strains expressing AAD genes were still higher than those by the TA-producing strains. Furthermore, under the conditions containing 10 or 25 mM of αKG, the TA-producing strains accumulated 180 μM of IAA, which is identical to the level accumulated by the AAD-producing strains.

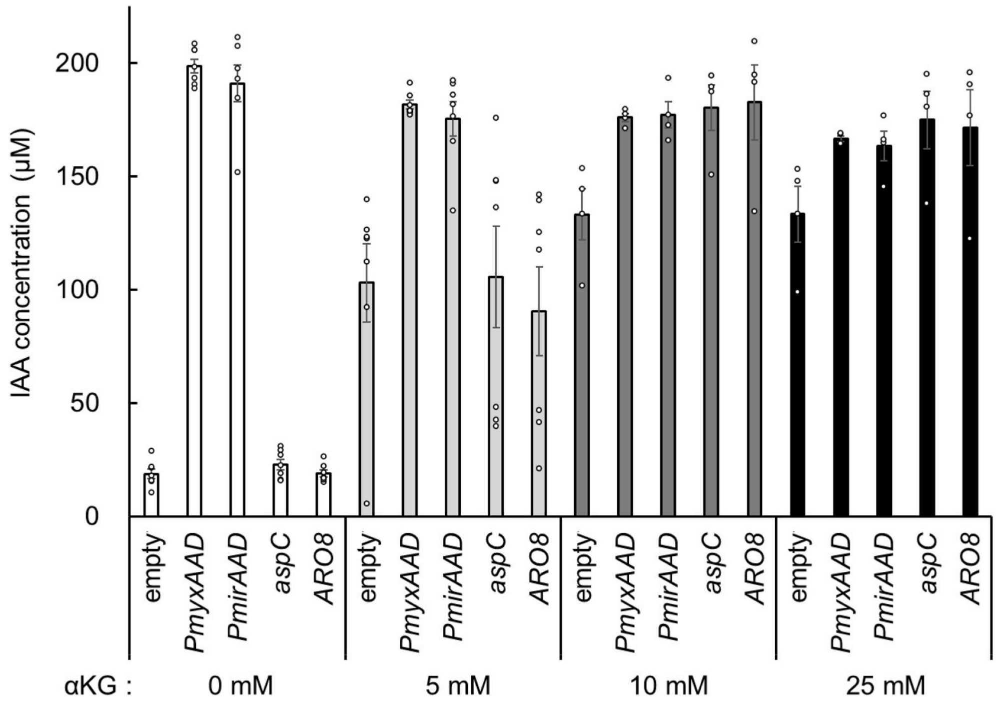

Fig. 5. IAA production by AAD- or TA-harboring strains. IAA production in culture supernatant of *E. coli* strains overexpressing AAD or TA genes, in combination with expression of *ipdC* and *puuC*, in the presence or absence of αKG. The values are means and standard errors of four independent experiments.

However, these conditions are not realistic situations. These results suggest that AADs are suitable enzymes to produce KAs or KA-derived compounds from AAs than TAs.

3.3. Kinetic analysis of AADs and TAs

It has been discussed that TA is not able to convert AAs to KAs so efficiently particularly in cell because it requires αKG, which is an important intermediate involved in several metabolic pathways. However, our bioconversion experiments indicated that AADs produced more IPA from tryptophan than TAs in *E. coli* cells even αKG was exogenously supplied, regardless of its concentration (Fig. 3A). This suggests that further mechanisms contribute to the superiority of AADs to TAs for KA production, in addition to the αKG independence of AADs. Therefore, we performed kinetic analyses of purified PmyxAAD and TAs to investigate additional mechanisms. The purified PmyxAAD, AspC, and Aro8 proteins exhibited almost single band in SDS-PAGE, indicating that they were pure enough for subsequent analyses (Fig. S1). Additionally, the purified PmyxAAD showed a characteristic UV-Vis spectrum, indicating the enzyme binding to its essential cofactor FAD (Fig. S2). As a result of our kinetic analysis, PmyxAAD exhibited 1.18 (±0.19) mM of K_m value to tryptophan, while K_m of Aro8 toward tryptophan was 5.00 (±0.52) mM (Fig. 6A and B). Furthermore, K_m of AspC was not determined because the activity of AspC increased as tryptophan concentration increased linearly in the range of tryptophan concentration tested here (Fig. 6B). This implies K_m value of AspC to tryptophan is much higher than 5 mM, which is the highest concentration of tryptophan used in this assay. These results indicate that AADs have higher affinity to tryptophan than TAs, which would contribute to the superior characteristics of AADs for IPA production from tryptophan in cell, regardless of αKG.

3.4. Bioconversion of other AAs to the corresponding KAs

To demonstrate the superiority of AADs to TAs as an enzyme to convert other AAs to KAs, we analyzed the bioconversion efficiency of AADs using other AAs as substrates. First, the substrate preference of the purified AADs towards 22 AAs was examined (Fig. S1 and 7). Both PmyxAAD and PmirAAD exhibited clear activity toward all of the tested AAs, with especially strong activity to aromatic and hydrophobic AAs. Such broad substrate selectivity of AADs were consistent with the previous study (Motta et al., 2016).

Subsequently, we measured and compared the bioconversion activity of AADs and TAs from phenylalanine, leucine, and valine to their

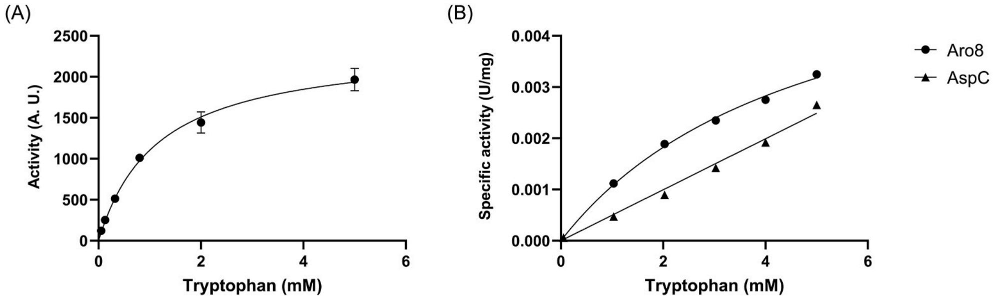

Fig. 6. Kinetic analysis of purified PmyxAAD, Aro8, and AspC. Michaelis-Menten plot of the purified (A) PmyxAAD, (B) Aro8, or AspC towards tryptophan. The values are means and standard errors of three independent experiments.

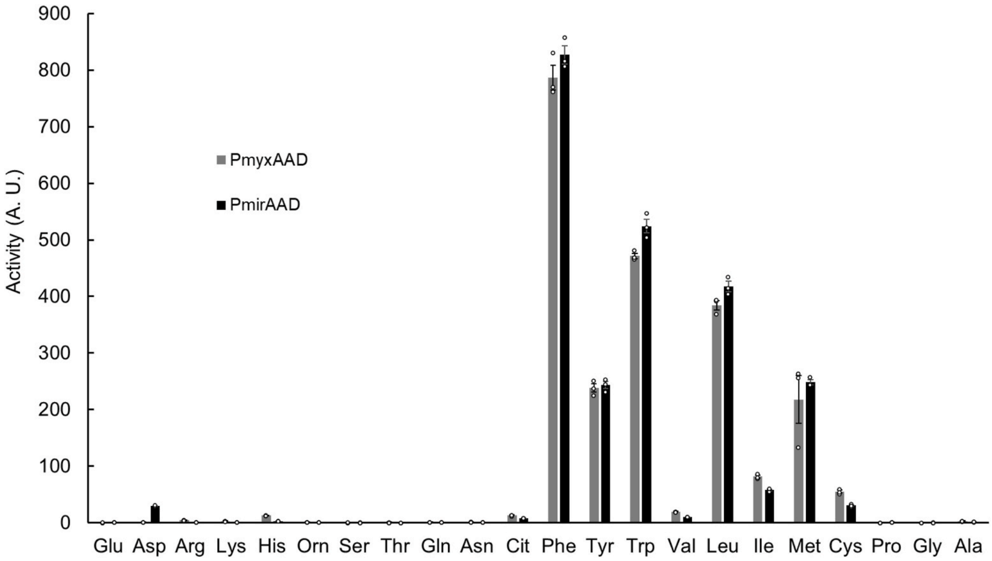

Fig. 7. AAD activity towards 22 amino acids. The enzymatic activity of the purified PmyxAAD (gray bar) and PmirAAD (black bar) towards 22 amino acids. Proteinogenic AAs are indicated in the usual three-letter code. Cit: citrulline, Orn: ornithine. Activity was expressed as an arbitrary unit (A. U.), calculated by normalizing the observed increment in fluorescence over time in the AAD assay by the protein level in the assay.

corresponding KAs. *E. coli* strain expressing *PmyxAAD* or *PmirAAD* produced around 540 or 340 μM Ppyv from phenylalanine, respectively, while cells expressing *tyrB*, which encodes an aromatic amino acid transaminase derived from *E. coli*, scarcely produced Ppyv in the absence of αKG, same as the empty vector-harboring strain (Fig. 8A). The addition of αKG altered the Ppyv production, however, the cells expressing AAD genes always exhibited the higher Ppyv accumulation than those expressing *tyrB*. Considering the protein level in cell shown by SDS-PAGF, the higher Ppyv production by the strain expressing AAD genes should be caused by their enzymatic properties but not the protein levels (Fig. 8B). These suggest that PmyxAAD and PmirAAD are more capable of producing Ppyv from phenylalanine than TyrB, regardless of αKG.

Using valine as a substrate, *E. coli* strains producing PmyxAAD or PmirAAD synthesized almost 290 or 230 μM KIV, while cells harboring an empty vector or expressing *ilvE* hardly synthesized KIV, without αKG supplementation (Fig. 8C). The addition of αKG increased the KIV accumulation of cells expressing *ilvE* and no significant differences were observed in the KIV production level between the strains expressing AAD genes and those expressing *ilvE* in the presence of 10, 20, or 50 mM of αKG. These suggest that AADs are suitable for converting valine to KIV because of their independence on αKG, while AADs would possess more capability for KIV production regardless of αKG, comparing the protein levels of PmyxAAD, PmirAAD, and TyrB in *E. coli* cell (Fig. 8B).

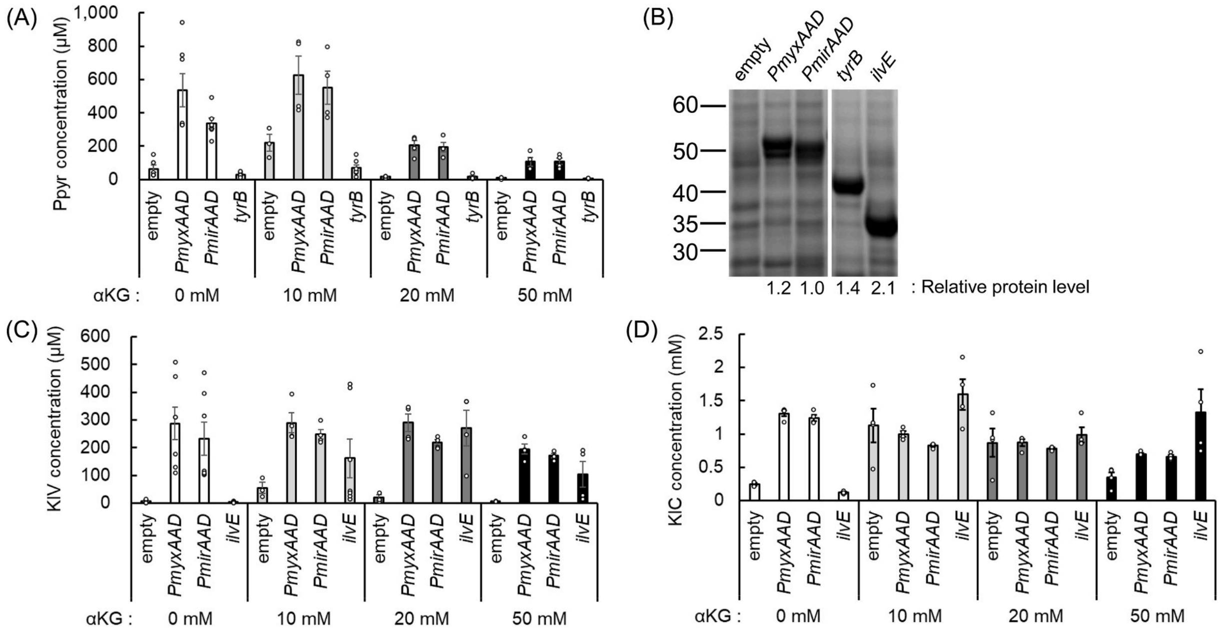

Fig. 8. Bioconversion of phenylalanine, leucine, and valine by strains expressing AAD- or TA-encoding gene. The corresponding KA production from (A) phenylalanine, (C) valine, and (D) leucine in culture supernatant of each strain, in the presence or absence of αKG. The values are means and standard errors of at least three independent experiments. (B) The protein level of each enzyme was demonstrated by SDS-PAGE. Empty indicate the cells harboring an empty vector. The protein level of each enzyme of interest (PmyxAAD, PmirAAD, TyrB, and IlvE) was quantified by densitometry using ImageJ and the relative protein levels were indicated.

When leucine was used as a substrate, *E. coli* expressing *PyxAAD* or *PmirAAD* produced more than 1.2 mM of KIC, while cells harboring an empty vector or those expressing the *ilvE* gene, which encodes a branched chain amino acid transaminase synthesized 0.2 or 0.1 mM of KIC, in the absence of αKG (Fig. 8C). The αKG supplementation drastically decreased the differences in KIC accumulation levels of each strains, cancelling the superiority of AAD to TA for KIC production; especially, the *ilvE*-expressing strain produced significantly higher concentration of KIC than the strain expressing PmyxAAD or PmirAAD. These suggest that AADs are superior to TAs for KIC production due to their independence from αKG.

These results imply that AADs are superior to TAs not only for IAA production but also for various KAs production from their precursors AAs, although the underlying mechanisms differ depending on the substrates AAs.

4. Discussion

Our kinetic analyses demonstrated that the affinity of PmyxAAD to its substrate tryptophan is higher than that of TAs, Aro8 and AspC. In contrast, TAs generally have more specific selectivity to the substrate AAs than AADs. For example, it has been shown that AspC or TyrB exhibited a clear activity to only five AAs, aspartate, glutamate, tryptophan, phenylalanine, and tyrosine among 17 proteinogenic AAs tested, whose catalytic efficiency k_{cat}/K_m were higher than 0.1% of that of their best substrate, aspartate or phenylalanine, respectively (Hayashi et al., 1993). Aro8 has been reported to convert four proteinogenic AAs to their corresponding KAs (Karsten et al., 2011). The previous study reported the transamination activity of IlvE toward five proteinogenic AAs with 0.1% or higher specific activity compared with that of its best substrate isoleucine (Lee-Peng et al., 1979). On the other hand, Motta et al., reported that PmyxAAD exhibited its enzymatic activity toward 17 AAs among 20 proteinogenic AAs with higher than 0.1% of specific activity compared to that of its most preferred substrate phenylalanine (Motta et al., 2016). Therefore, AAD is an enzyme harboring both high affinity and broad selectivity, which appear to be contradictory in nature each other at first glance. It could be that AAD strongly recognizes and binds to the common moiety of its substrate AAs, such as α-carboxylic and α-amino groups, while the recognition of side chain is relatively loose, even though the 3D structure of AAD bound to its substrate has not been determined experimentally.

We showed that the higher affinity of AADs than TAs made AADs superior to TAs for KAs production, in addition to that TAs require αKG as an amino group acceptor. However, considering the reaction mechanisms and characteristics of each enzyme, further mechanisms for AADs' superiority could be raised. TAs catalyzes the reversible transamination between AAs and KAs, in contrast the reaction by AADs is irreversible. Therefore, the intracellular concentration of glutamate, which is a byproduct of transamination reaction from AAs to αKG catalyzed by TAs, should affect the conversion rate from AAs to the corresponding KAs and also total yield of final products. AAOs also catalyze the irreversible reaction, however, the cytotoxicity mediated by their byproduct H_2O_2 is an important issue to be addressed. Totally, AADs would be most suitable for the production of KAs from AAs among the metabolic enzymes reported so far.

Here, we developed high throughput assay system to measure the AAD activity using mPES and resazurin as an electron mediator and a fluorescence electron probe, respectively. The measurement system to analyze the enzymatic activity of oxidoreductase by monitoring the absorbance at 340 nm derived from NAD(P)H has been used for many kinds of enzymes. However, this method is suitable only for enzymes using $NAD(P)^+$ or NAD(P)H. Our developed methods are suitable for all enzymes catalyzing oxidative reactions theoretically.

For Bioproduction, too broad substrate selectivity of enzymes used for designed pathways would have adverse effects by unexpectedly affecting metabolic pathways. Therefore, one of the potential problems to be solved in the usage of AADs for KA production is an enzyme promiscuity of AAD reaction. In this study, though no quantitative growth analysis was performed, no apparent growth defect was observed upon AAD gene overexpression under the conditions tested. However, various AAs other than tryptophan would be metabolized by PmyxAAD and PmirAAD during IAA production, potentially resulting in AA starvation and resultant growth defect. Our IAA production assay was performed in LB medium containing various AAs and peptides, which protects cells from starving AAs. When cells producing AADs were cultured in minimal medium and/or the activity of AADs were highly enhanced by engineering, the promiscuity of AADs is potential to exert cytotoxicity or lead to growth defects. Engineering to increase not only enzymatic activity but also substrate specificity to its target AA is highly desired for further usage of AADs for bioproduction.

5. Conclusions

In this study, we demonstrated that AADs are more suitable to synthesize KAs or their related compounds from the corresponding AAs than TAs experimentally. We also indicated that the αKG independence and/or the higher substrate affinity of AADs contributes to AAD's superiority to TAs. To our best knowledge, this is the first report to demonstrate the superiority of AADs to TAs for the production of KAs and its mechanisms. Our results should contribute to rational enzyme selection for KA biosynthetic pathways.

CRediT authorship contribution statement

Ryo Nasuno: Writing – review & editing, Writing – original draft, Visualization, Validation, Methodology, Investigation, Formal analysis, Conceptualization. **Hisashi Kudo:** Methodology, Investigation, Formal analysis. **Keiji Fushimi:** Visualization, Conceptualization. **Ryota Hidese:** Writing – review & editing. **Akihiko Kondo:** Resources, Project administration, Funding acquisition. **Tomohisa Hasunuma:** Writing – review & editing, Supervision, Resources, Project administration, Funding acquisition, Conceptualization.

Declaration of competing interest

The authors declare no competing financial interests.

Acknowledgments

We thank Ms. Yuka Oda, Ms. Mio Hayama, Ms. Eriko Shibayama, and Mr. Keiichiro Kami for their technical assistance. This work was supported by NEDO Projects P20011 (Development of bioderived product production technology that accelerates the realization of carbon recycling). It was also supported by the Program for Forming Japan's Peak Research Universities (J-PEAKS) Grant Number JPJS00420230009 from the Japan Society for the Promotion of Science (JSPS).

Appendix A. Supplementary data

Supplementary data to this article can be found online at https://doi.org/10.1016/j.ymben.2026.04.001.

Data availability

Data will be made available on request.

References

Atsumi, S., Hanai, T., Liao, J.C., 2008. Non-fermentative pathways for synthesis of branched-chain higher alcohols as biofuels. Nature 451, 86–89. https://doi.org/10.1038/nature06450.

Atsumi, S., Wu, T.Y., Eckl, E.M., Hawkins, S.D., Buelter, T., Liao, J.C., 2010. Engineering the isobutanol biosynthetic pathway in Escherichia coli by comparison of three aldehyde reductase/alcohol dehydrogenase genes. Appl. Microbiol. Biotechnol. 85, 651–657. https://doi.org/10.1007/s00253-009-2085-6.

Cowan, A.E., Klass, S.H., Winegar, P.H., Keasling, J.D., 2023. Microbial production of fuels, commodity chemicals, and materials from sustainable sources of carbon and energy. Curr. Opin. Syst. Biol. 36, 100482. https://doi.org/10.1016/j.coisb.2023.100482.

Fujiwara, T., Hattori, A., Ito, T., Funatsu, T., Tsunoda, M., 2020. Analysis of intracellular α-keto acids by HPLC with fluorescence detection. Anal. Methods 12, 2555–2559. https://doi.org/10.1039/d0ay00556h.

Gu, P., Zhao, S., Niu, H., Li, C., Jiang, S., Zhou, H., Li, Q., 2023. Synthesis of isobutanol using acetate as sole carbon source in Escherichia coli. Microb. Cell Fact. 22, 196. https://doi.org/10.1186/s12934-023-02197-w.

Guo, D., Kong, S., Chu, X., Li, X., Pan, H., 2019. De novo biosynthesis of indole-3-acetic acid in engineered escherichia coli. J. Agric. Food Chem. 67, 8186–8190. https://doi.org/10.1021/acs.jafc.9b02048.

Ha, K., Ryu, S., Trinh, C.T., 2025. Alpha-ketoacid decarboxylases: diversity, structures, reaction mechanisms, and applications for biomanufacturing of platform chemicals and fuels. Biotechnol. Adv. 81, 108531. https://doi.org/10.1016/j.biotechadv.2025.108531.

Hasegawa, S., Jojima, T., Suda, M., Inui, M., 2020. Isobutanol production in Corynebacterium glutamicum: suppressed succinate by-production by pckA inactivation and enhanced productivity via the Entner–Doudoroff pathway. Metab. Eng. 59, 24–35. https://doi.org/10.1016/j.ymben.2020.01.004.

Hayashi, H., Inoue, K., Nagata, T., Kuramitsu, S., Kagamiyama, H., 1993. Escherichia coli aromatic amino acid aminotransferase: characterization and comparison with Aspartate aminotransferase. Biochemistry 32, 12229–12239. https://doi.org/10.1021/bi00096a036.

Hossain, G.S., Li, J., Shin, H.D., Du, G., Wang, M., Liu, L., Chen, J., 2014. One-step biosynthesis of α-keto-γ- Methylthiobutyric acid from l-methionine by an Escherichia coli whole-cell biocatalyst expressing an engineered lamino acid deaminase from proteus vulgaris. PLoS One 9, e114291. https://doi.org/10.1371/journal.pone.0114291.

Hou, Y., Hossain, G.S., Li, J., Shin, H. dong, Du, G., Liu, L., 2016. Combination of phenylpyruvic acid (PPA) pathway engineering and molecular engineering of l-amino acid deaminase improves PPA production with an Escherichia coli whole-cell biocatalyst. Appl. Microbiol. Biotechnol. 100, 2183–2191. https://doi.org/10.1007/s00253-015-7048-5.

Karsten, W.E., Reyes, Z.L., Bobyk, K.D., Cook, P.F., Chooback, L., 2011. Mechanism of the aromatic aminotransferase encoded by the Aro8 gene from Saccharomyces cerevisiae. Arch. Biochem. Biophys. 516, 67–74. https://doi.org/10.1016/j.abb.2011.09.008.

Koper, K., Han, S.W., Pastor, D.C., Yoshikuni, Y., Maeda, H.A., 2022. Evolutionary origin and functional diversification of aminotransferases. J. Biol. Chem. 298, 102122. https://doi.org/10.1016/j.jbc.2022.102122.

Lee-Peng, F.C., Hermodson, M.A., Kohlhaw, G.B., 1979. Transaminase B from Escherichia coli: quaternary structure, amino-terminal sequence, substrate specificity, and absence of a separate valine-α-ketoglutarate activity. J. Bacteriol. 139, 339–345. https://doi.org/10.1128/jb.139.2.339-345.1979.

Li, Y., Ogola, H.J.O., Sawa, Y., 2012. L-Aspartate dehydrogenase: features and applications. Appl. Microbiol. Biotechnol. 93, 503–516. https://doi.org/10.1007/s00253-011-3730-4.

Liu, H., Tian, M., Dong, P., Zhao, Y., Deng, Y., 2025. Metabolic engineering of Escherichia coli for the improved malonic acid production. ACS Synth. Biol. 14, 1277–1287. https://doi.org/10.1021/acssynbio.5c00005.

Marsh, E.N.G., Waugh, M.W., 2013. Aldehyde decarbonylases: enigmatic enzymes of hydrocarbon biosynthesis. ACS Catal. 3, 2515–2521. https://doi.org/10.1021/cs400637t.

Molla, G., Melis, R., Pollegioni, L., 2017. Breaking the mirror: L-Amino acid deaminase, a novel stereoselective biocatalyst. Biotechnol. Adv. 35, 657–668. https://doi.org/10.1016/j.biotechadv.2017.07.011.

Motta, P., Molla, G., Pollegioni, L., Nardini, M., 2016. Structure-function relationships in L-amino acid deaminase, a flavoprotein belonging to a novel class of biotechnologically relevant enzymes. J. Biol. Chem. 291, 10457–10475. https://doi.org/10.1074/jbc.M115.703819.

Nasuno, R., Hirano, Y., Itoh, T., Hakoshima, T., Hibi, T., Takagi, H., 2013. Structural and functional analysis of the yeast n-Acetyltransferase mpr1 involved in oxidative stress tolerance via proline metabolism. Proc. Natl. Acad. Sci. U. S. A 110, 11821–11826. https://doi.org/10.1073/pnas.1300558110.

Nieto-Domínguez, M., Sako, A., Enemark-Rasmussen, K., Gotfredsen, C.H., Rago, D., Nikel, P.I., 2024. Enzymatic synthesis of mono- and trifluorinated alanine enantiomers expands the scope of fluorine biocatalysis. Commun. Chem. 7, 104. https://doi.org/10.1038/s42004-024-01188-1.

Pollegioni, L., Motta, P., Molla, G., 2013. L-Amino acid oxidase as biocatalyst: a dream too far? Appl. Microbiol. Biotechnol. 97, 9323–9341. https://doi.org/10.1007/s00253-013-5230-1.

Romasi, E.F., Lee, J., 2013. Development of indole-3-acetic acid-producing Escherichia coli by functional expression of IpdC, AspC, and Iad1. J. Microbiol. Biotechnol. 23, 1726–1736. https://doi.org/10.4014/jmb.1308.08082.

Rumpl, A.E.C., Goodhew, J.R., Kelly, P.F., Hirano, M., Pyne, M.E., 2025. Brews, fuels, and opioids: expanding the yeast Ehrlich pathway for chemical and pharmaceutical manufacturing. Biotechnol. Adv. 84, 108684. https://doi.org/10.1016/j.biotechadv.2025.108684.

Schneider, C.A., Rasband, W.S., Eliceiri, K.W., 2012. NIH Image to ImageJ: 25 years of image analysis. Nat. Methods 9, 671–675. https://doi.org/10.1038/nmeth.2089.

Schriek, S., Kahmann, U., Staiger, D., Pistorius, E.K., Michel, K.P., 2009. Detection of an L-amino acid dehydrogenase activity in Synechocystis sp. PCC 6803. J. Exp. Bot. 60, 1035–1046. https://doi.org/10.1093/jxb/ern352.

Smith, A.B., Chekan, J.R., 2023. Engineering yeast for industrial-level production of the antimalarial drug artemisinin. Trends Biotechnol. 41, 267–269. https://doi.org/10.1016/j.tibtech.2022.12.007.

Smith, H.Q., Li, C., Stanley, C.A., Smith, T.J., 2019. Glutamate dehydrogenase, a complex enzyme at a crucial metabolic branch point. Neurochem. Res. 44, 117–132. https://doi.org/10.1007/s11064-017-2428-0.

Song, Y., Li, J., Shin, H. dong, Liu, L., Du, G., Chen, J., 2016. Biotechnological production of alpha-keto acids: current status and perspectives. Bioresour. Technol. 219, 716–724. https://doi.org/10.1016/j.biortech.2016.08.015.

Tashiro, Y., Rodriguez, G.M., Atsumi, S., 2015. 2-Keto acids based biosynthesis pathways for renewable fuels and chemicals. J. Ind. Microbiol. Biotechnol. 42, 361–373. https://doi.org/10.1007/s10295-014-1547-8.

Wendisch, V.F., Jorge, J.M.P., Pérez-García, F., Sgobba, E., 2016. Updates on industrial production of amino acids using Corynebacterium glutamicum. World J. Microbiol. Biotechnol. 32, 105. https://doi.org/10.1007/s11274-016-2060-1.

Wess, J., Brinek, M., Boles, E., 2019. Improving isobutanol production with the yeast Saccharomyces cerevisiae by successively blocking competing metabolic pathways as well as ethanol and glycerol formation. Biotechnol. Biofuels 12, 173. https://doi.org/10.1186/s13068-019-1486-8.

Wong, N., Jantama, K., 2022. Engineering Escherichia coli for a high yield of 1,3-propanediol near the theoretical maximum through chromosomal integration and gene deletion. Appl. Microbiol. Biotechnol. 106, 2937–2951. https://doi.org/10.1007/s00253-022-11898-y.

Zhang, K., Woodruff, A.P., Xiong, M., Zhou, J., Dhande, Y.K., 2011. A synthetic metabolic pathway for production of the platform chemical isobutyric acid. ChemSusChem 4, 1068–1070. https://doi.org/10.1002/cssc.201100045.

Zheng, X., Liu, Y., Li, Y., Wang, Y., Yang, X., 2024. De Novo Biosynthesis of 2-Phenylethanol by Metabolic Engineering the Oleaginous Yeast Rhodotorula toruloides. J. Agric. Food Chem. 72, 26777–26785. https://doi.org/10.1021/acs.jafc.4c07705.